Scripta Materialia 157 (2018) 162–166

Contents lists available at ScienceDirect

Scripta Materialia

journal homepage: www.elsevier.com/locate/scriptamat

Regular article

Examining the influence of stacking fault width on deformation twinning in an austenitic stainless steel

G. Meric de Bellefon [a,*], M.N. Gussev [b], A.D. Stoica [b], J.C. van Duysen [c,d,e], K. Sridharan [a,f]

[a] Department of Engineering Physics, University of Wisconsin, Madison, USA
[b] Oak Ridge National Laboratory, Oak Ridge, USA
[c] Unité Matériaux et Transformation (UMET) CNRS, Université de Lille 1, France
[d] Department of Nuclear Engineering, University of Tennessee, Knoxville, USA
[e] EDF—Centre de Recherche des Renardieres, Moret sur Loing, France
[f] Department of Materials Science and Engineering, University of Wisconsin, Madison, USA

ARTICLE INFO

Article history:
Received 11 June 2018
Received in revised form 21 July 2018
Accepted 9 August 2018
Available online xxxx

Keywords:
Austenitic 316 stainless steel
Deformation twinning
Stacking fault energy
Neutron diffraction

ABSTRACT

Two austenitic stainless steels (SS) were designed to exhibit close to the largest possible difference in stacking fault energy (SFE) while staying within specifications. Neutron diffraction and scanning electron microscopy electron backscatter diffraction analysis were used to quantify stacking fault widths and deformation twinning, respectively, during room temperature straining. While the low-SFE SS exhibits much wider stacking faults (19 nm) throughout deformation as compared to the high-SFE SS (12 nm), the difference in twinning is less pronounced, with a slightly lower stress (50–100 MPa lower) and lower strain (5–10%) for twinning onset in the low-SFE SS.

Since its development in the early 1900s, 316 austenitic stainless steel (316 SS) has been relied upon for many applications because of its good corrosion resistance and mechanical properties, and relatively low cost. The specification for 316 SS allows ample variation in the composition, in particular in Ni (10 to 14 wt%) and Cr (16 to 18 wt%) contents. Understanding the influence of alloying elements on deformation mechanisms of 316 SS can be used to define compositions that lead to mechanical properties tailored to specific applications. One parameter that may be used to predict deformation mechanisms is the stacking fault energy (SFE). Trends in experimental data on FeMnC steels [1] and SS [2] have led some authors [3,4] to propose ranges of SFE correlated to certain dominant deformation mechanism in fcc metals and alloys: 15–18 mJ/m^2 < SFE < 50 mJ/m^2 for twinning, SFE < 15–18 mJ/m^2 for deformation-induced martensite, and 50 mJ/m^2 < SFE for slip-based plasticity. Existing SFE measurements and expressions to calculate SFE from composition in SS exhibit a wide range of values. For 316 SS, for example, values ranging between 14.2 mJ/m^2 [5] and 78 ± 6 mJ/m^2 [6] have been measured at room temperature (RT), and, until recently, expressions to predict SFE showed an even wider range of SFE [7]. As detailed in [7], an analysis of the entire database of available SFE measurements in FeNiCr alloys shows that the possible range of SFE is likely 20 to 35 mJ/m^2 for 316 SS. The question of whether such a variation in SFE affects the deformation behavior of 316 SS is explored here.

In the present work, two 316 SS compositions were selected to exhibit close to the largest possible difference in SFE while still staying within compositional specification (see Table 1). The stress-strain curves of the two steels are shown in Fig. 1. Both steels were strained at RT in a neutron diffractometer to quantify the influence of composition on stacking fault width. The influence of composition on twinning was then investigated through interrupted tensile tests at RT followed by SEM EBSD. Special care was given to separate the effects of grain size and composition.

In situ tensile tests with neutron diffraction were conducted at the engineering time-of-flight neutron diffractometer VULCAN facility at Oak Ridge National Laboratory [8–10]. VULCAN's standard 3-mm gauge flat tension sample geometry was used. The high-intensity mode was employed at 30 Hz repetition rate, corresponding to a 0.6–3.4 Å wavelength range. Neutrons were scattered by the entire thickness of the samples encompassing a volume of about 7 × 3 × 4 mm. Only the {hkl} reflections into the detector bank corresponding to the loading direction (LD) were used in this work, which correspond to grains having an ⟨hkl⟩ direction aligned with LD [11]. Diffraction data was recorded during tensile testing at RT under load control mode up to the yield point, followed by 1.2 × 10^{-3} s^{-1} strain rate displacement controled mode with 5 min interruptions at every 2% strain increment for neutron data collection. Images of the strained specimens were

* Corresponding author.
E-mail address: mericdebelle@wisc.edu (G. Meric de Bellefon).

https://doi.org/10.1016/j.scriptamat.2018.08.012
1359-6462/

Table 1
Elemental composition (wt%), annealing treatment, grain size and ferrite content of the two 316 stainless steels used in this study.

Alloy	Ni	Cr	Mo	Mn	Si	C	N	Calculated SFE from formula in [7]*	Annealing	Average grain size	δ ferrite fraction
316#1	10	18	3.0	0.94	0.77	0.003	0.006	22 mJ/m^2	1100 °C 60 min	≈15 μm	≈5 vol%
316#2	14	18	3.0	0.94	0.10	0.04	0.009	33 mJ/m^2	1000 °C 30 min	≈25 μm	0

* In the low-SFE alloy, the presence of ferrite did not noticeably change the austenite phase composition from the nominal compsition, as measured with Energy Dispersive X-Ray Spectroscopy.

recorded to estimate true stress/strain curves through digital image correlation [12]. Diffraction data was analyzed with the software VDRIVE [13] and the Single Peak Fitting function based on GSAS TOF profile function 3 [14]. It relies in particular on the pseudo-Voigt approximation [15], which considers the sum of a Gaussian component and a Lorentzian component as the peak profile. Fitting of two pairs of fcc peaks, {111}/{222} and {200}/{400}, are used in this work. The output of single peak fitting includes the peak position d_{hkl}, the peak intensity I_{hkl}, and the peak broadening, characterized by the full width at half maximum (FWHM) of the full peak, Γ_{hkl}, and its Gaussian, Γ^G_{hkl}, and Lorentzian, Γ^L_{hkl}, components. Diffraction peak shifts are attributed to lattice strains or a change in d-spacing, which represent the elastic deformation of the lattice under load. As the strain is a relative number, it should not depend of the order of reflection (e.g., {111}, {222}). However, there are some other causes of peak shifting - one peculiar type of crystallographic defect able to induce distinctive peak shifts is the staking fault. In fcc materials such as SS, stacking faults occur in the packing of {111} planes. The influence of stacking faults on diffraction patterns was first investigated by Warren [16]. According to Warren's theory, stacking faults induce a peak shift of high order diffraction peaks, {nh,nk,nl}, relative to the primary reflection, {hkl}. The {hkl} peak relative shift is proportional to the surface fraction of stacking faults in {111} planes, called stacking fault probability, P_{SF}, and the Warren's factors [16], η_{hkl}:

$$\left(\frac{\Delta d_{SF}}{d}\right)_{hkl} = -\frac{\sqrt{3}}{4\pi}\eta_{hkl}P_{SF} \tag{1}$$

As the η_{hkl} factors are different for {111} and {222} reflections (1/4 for {111} and −1/8 for {222}), the presence of stacking faults induces an apparent difference in lattice strain between {111} and {222} (see Fig. 2(a)). Since the (real) elastic lattice strain is equal for {111} and {222}, the difference in total relative shift between {111} and {222} is equal to the difference in stacking fault-induced peak shift. Hence, P_{SF} for ⟨111⟩ grains (i.e., grains with a ⟨111⟩ direction aligned with LD) is given by:

$$P_{SF,111} = \frac{1}{0.051}\left(\frac{\Delta d}{d}_{222} - \frac{\Delta d}{d}_{111}\right) \tag{2}$$

The same procedure can be applied for ⟨100⟩ grains with the pair {200}–{400} (see Fig. 2(b)).

For each strain step, the dislocation density was estimated by using Wilkens analytical model [17] under the approximation proposed in [18]:

$$\beta = \frac{b\sqrt{C\rho}}{F\left(e^{2\pi}b\sqrt{\rho}\right)} \tag{3}$$

with β: integral breadth, b: Burgers vector of perfect dislocations (b = $a_0/2$ ⟨110⟩), C: ⟨hkl⟩-dependent dislocation contrast factor, ρ: perfect dislocation density, F: defined by $F(M) = 2M\int_0^\infty e^{-\frac{\pi}{2}M^2x^2}f(x)dx$, and f (x) the Wilkens profile function [17]. The contrast factors were calculated with the ANIZC software [19] and the function F was numerically estimated. Only the integral breath contribution from sample deformation (SD) β^{SD} was used - it was calculated from the output of the single peak fitting by using the total FWHM, Γ^{SD}, and the relative weight of Lorentz component, η, as follows:

$$\beta^{SD} = \frac{\Gamma^{SD}}{2}\left[\sqrt{\frac{\ln 2}{\pi}} - \left(\sqrt{\frac{\ln 2}{\pi}} - \frac{1}{\pi}\right)\eta\right]^{-1} \tag{4}$$

The equations for calculating Γ^{SD} and η from Γ^G_{hkl} and Γ^L_{hkl} are given in [14,15]. The SD contributions were estimated by subtracting the zero-strain FWHM values: $\Gamma^{G,SD} = \sqrt{(\Gamma^G)^2 - (\Gamma^{G,0})^2}$ and $\Gamma^{L,SD} = \Gamma^L - \Gamma^{L,0}$.

The stacking fault width can be estimated using the relationship between perfect dislocation density ρ and average dissociation width w [20]:

$$P_{SF} = \frac{\rho w a_0}{\sqrt{3}} \tag{5}$$

with a_0 the lattice parameter. The evolution of stacking fault probability in ⟨111⟩ and ⟨100⟩ grains with dislocation density in those grains for 316#1 and 316#2 at RT is shown in Fig. 3(a) and (b). A linear trend is observed when plotting stacking fault probability against dislocation density - the slope of the linear fit gives an estimation of the stacking fault width. The curves overlap for ⟨111⟩ and ⟨100⟩ grains, indicating that stacking fault widths are similar in both grain families. Using a_0 = 0.36 nm, we find average separation distances of 19 nm and 12 nm for 316#1 and 316#2, respectively. The grain size or the presence of ferrite inclusion is not expected to affect the stacking fault width; transmission electron microscopy examination confirmed no influence of grain boundaries on stacking fault widths.

For each SS, three additional tensile tests using the SS-J3 specimen geometry [21] were conducted and interrupted at three stress levels (about 663 MPa, 690 MPa, and 806 MPa for 316#1, and about 677 MPa, 720 MPa, and 840 MPa for 316#2). Samples for SEM

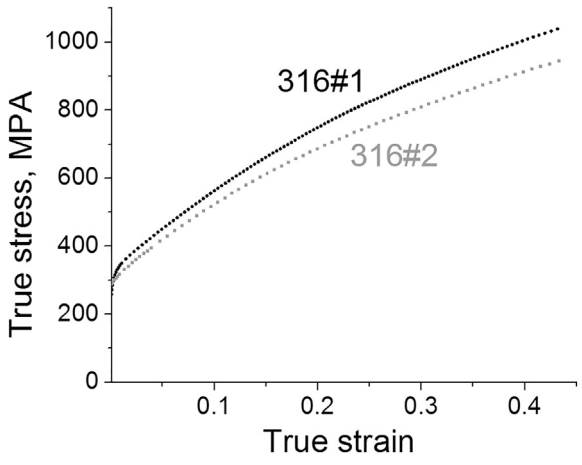

Fig. 1. True stress/trues strain curves for the two tested 316 SS.